Synthesis of textured complex backgrounds

Jannick P. Rolland
Alexei A. Goon
Liyun Yu
University of Central Florida
Center for Research and Education in Optics and Lasers
Orlando, Florida 32816
E-mail: rolland@creol.ucf.edu

Abstract. The statistical characterization of realistic, complex backgrounds where targets may be embedded is essential in the optimization of methods for target acquisition. A modeling framework for complex backgrounds that yields perceptually realistic images may provide a path towards such essential characterizations. To this end, we developed a framework for the synthesis of statistical textured backgrounds. The results of the syntheses of three rock-like structures and that of grass indicate some of the capabilities of the framework. We further extended the methods to synthesize biological tissue samples which present two forms of background complexity: a slowly, spatially varying mean-background and a residual texture image. The extended framework allows synthesis of each component independently. A mathematical phantom for modeling inhomogeneous backgrounds is then proposed. First and second order statistics of various textures are then presented and a measure of distance between two images is proposed. Finally we discuss how such a framework may lead to effective statistical descriptions of such complex backgrounds for target acquisition. [S0091-3286(98)01807-8]

Subject terms: textured backgrounds; complex backgrounds; texture synthesis; first and second order statistics; detection.

Paper TAM-18 received Dec. 12, 1997; revised manuscript received Feb. 24, 1998; accepted for publication Feb. 24, 1998.

1 Introduction

Research in imaging aims to create better imaging systems, and to develop methods of image processing and analysis that utilize the most important information present in an image. In the case of target acquisition in natural backgrounds, such methods are required for accurate and timely detection of relevant targets. Realistic numerical models of complex backgrounds as well as models of imaging systems are key components to achieving these goals. In this paper, we present a framework for synthesizing three types of complex statistical backgrounds: lumpy backgrounds, statistical textured backgrounds, or a combination of the two. Lumpy backgrounds denote specifically slowly varying backgrounds that are wide-sense stationary and present a Gaussian autocorrelation function.[1–3] Statistical textures are textures that present no apparent periodic pattern.

Texture synthesis is the ability to generate from one sample texture image a statistical ensemble of texture images. One synthetic image is a realization of the underlying random process that could be employed to generate the texture. While texture synthesis finds applications in computer graphics where textured scenes bring additional simulation realism, we hope to demonstrate that texture synthesis also finds important application to the domains of imaging and image analysis, which require models of complex background images.[4–8] Progress in image understanding and effective analysis requires the specification of a task. The task of target detection and classification in complex statistical backgrounds is the focus of the work presented here.

A synthesis framework that accounts for slowly varying backgrounds as well as smaller scale statistical textures leads to a digital complex-background phantom that may find important use in the development of methods for the optimization of target acquisition in complex backgrounds. We demonstrate synthesis methods with statistical textured backgrounds such as three types of rock and grass images. We further show synthesis of even more complex backgrounds such as radiological breast tissues. Radiological tissues are more complex in the sense that they include various types of statistical textures that have failed to be synthesized by existing methods. However we demonstrated in a recent investigation that they can be decomposed effectively into the sum of a slowly varying mean background, which we have proposed to model using lumpy backgrounds, and a statistical texture.[9] Breast tissue images thus provide good images to investigate a proposed framework that accounts for these two kinds of statistics.

It is important to note that current methods for detection of lesions in complex medical backgrounds were originally based on methods developed for target acquisition in radar images developed in the 1960's. The cases of lesion detection in medical and biomedical images, as well as that of military target acquisition, involve targets embedded in complex backgrounds that require "economical" statistical descriptions for the development of figures of merits for effective target detection and more generally target classification. While we are currently investigating such statistical descriptions, we shall present a framework for texture synthesis as well as its application to five texture types. We shall present results of first and second order statistical descriptions for those textures and propose a measure of distance between two images. We shall finally discuss how a

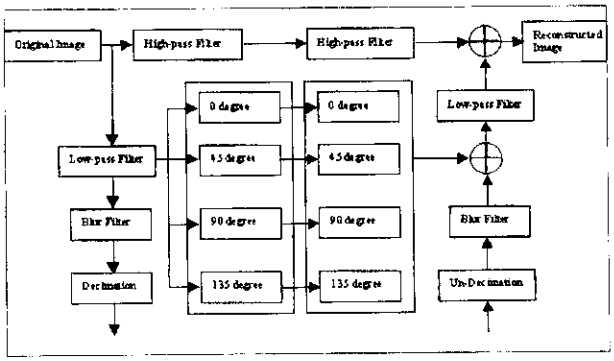

Fig. 1 Illustration of the steerable pyramid transform used in the texture synthesis algorithm. The input image in the upper left corner would be either the texture sample or the white noise image. The output image in the upper right corner will be either the reconstruction of a decomposed image if only one input image is considered, or a synthesis image if two pyramid layers are combined as described in Section 4. The left hand side of the pyramid is used for decomposing the two images and the right hand side of the pyramid is used for image reconstruction or synthesis.

synthesis framework may help unravel effective statistical descriptions of such complex backgrounds.

2 A Framework for Texture Synthesis

The algorithm for texture synthesis we propose is based on a multiple scale decomposition of a sample texture image and the same decomposition of a realization of a uniformly distributed white noise image. The algorithm is composed of four essential components: the pyramid transform, the image decomposition, the histogram matching procedure, and the texture synthesis. Texture synthesis based on a multiscale and multiorientation decomposition followed by histogram matching of the decomposed images was first proposed by Heeger and Bergen.[10] The algorithm we propose, depicted for one scale level in Fig. 1, includes a recursive steerable pyramid transform with a set of quadrature mirror filter banks.[11–14] By recursive we mean that once a first synthesis is obtained through the steerable pyramid, we reapply the algorithm but using the original sample texture and the last synthesis instead of the noise image first considered. The algorithm for one iteration employs a four-layer scale-space decomposition. In previously related cited work an overall description of the algorithm was given but various specifics were not provided (e.g. filter sizes, the number of scale levels considered in the pyramid description, details of decimation and undecimation). The decomposition of the images yields subband images that are processed independently. The histograms of the subband images of the model and the noise are then matched. After multiscale and multiorientation decomposition and histogram matching at all scales and orientations, the noise subband images are recombined using a quadrature mirror filter bank to yield a synthetic image.

The algorithm was implemented in IDL language and is best described by considering the four individual components:

The Pyramid Transform. The proposed algorithm for the synthesis of the residual texture is based on a four-layer steerable pyramid transform. One layer of the pyramid is depicted in Fig. 1. Layers are connected by a factor-of-two downsampling also known as decimation of the image.[15] Within each layer, the image is filtered by a set of bandpass filters and followed by a set of orientation filters that form a quadrature mirror filter bank.[15–17] Four (scales) by four (orientations: 0 degree, 45 degree, 90 degree and 135 degree) 17×17 size filters were adopted.

Image Decomposition. The texture image is processed through the left hand side of the pyramid transform shown in Fig. 1. It is represented in Fig. 1 as an input to the pyramid in the upper left corner. In parallel, a realization of uniformly distributed white noise, referred thereafter as white noise, is also processed by the same pyramid transform, that is, it is also fed independently to the pyramid transform in the upper left corner. The role of the white noise image is to provide a starting point for the synthesis.

Histogram Matching at Multiple Scales. After decomposition of a texture sample and a realization image of white noise, the histograms of the subband images (i.e. output images of the filters on the left hand side of the pyramid) of the texture image and of the noise image are matched.[14] Histogram matching is an image processing technique, specifically a point operation, which modifies a candidate image so that its histogram matches that of a model image.[18–20]

Texture Synthesis. The histogram-matched noise subband images obtained at multiple scales are then recombined according to the right hand side of the pyramid transform shown in Fig. 1. The synthesis operation is a bottom-up reconstruction that includes upsampling by a factor of two, also known as undecimation, and Gaussian blur between scales. Moreover, the grey levels of the undecimated image must be multiplied by a factor of four at each stage of the synthesis to account for the loss in brightness the image previously underwent upon decimation by a level of two. This process repeated at multiple scales yields a synthetic image. If another realization of white noise is processed instead, the synthesis yields another realization of the synthesized image as shown in Section 3.

3 Examples of Texture Synthesis of Natural Structures

Application of the texture synthesis framework is demonstrated in Figs. 2 and 3 for four different model texture images: three different granite samples and a grass sample. The original samples and the synthesized images are shown as well as their histograms. Two realizations of image synthesis were generated for each texture of model using two different realizations of the noise input image that was chosen to be uniformly distributed white noise. The framework was extended to allow for the synthesis of biological samples. We investigated the specific application of texture synthesis of mammogram images. Based on our experience, application of the steerable pyramid transform to mammogram images does not yield perceptually resembling mammograms.[21] A two-component model synthesis framework to handle more complex backgrounds such as, but not limited to, mammograms is now described.

4 A Two-Component Model Synthesis Framework

Investigations of the statistics of texture backgrounds may guide approaches to their synthesis. It has been suggested

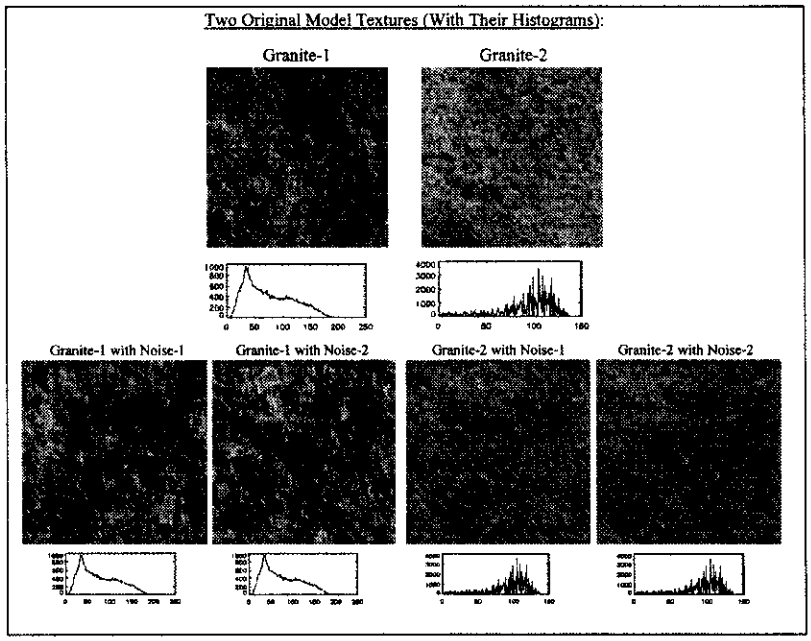

Fig. 2 Results of texture synthesis for two textures denoted as Granite-1 and Granite-2. The histograms of the original samples as well as of the syntheses for two realizations of uniformly distributed white noise are shown.

that various classes of images, including mammograms, have power spectra of the form $1/f^{\alpha}$.[22–25] For mammograms, estimated values of α in the range of 1.5 to 2 have been reported.[24,25] A power-law spectrum exponent between 1.5 and 2 indicates that mammograms are not fractals. A two-dimensional fractal would yield an exponent greater than 2. This finding further suggests that such backgrounds cannot be synthesized using fractals.[26] Therefore, while some investigations have demonstrated that different mammographic tissue types can be classified according to their estimated fractal dimension,[23] some of these investigations have further demonstrated that the addition of another parameter significantly yields improved classification.[25,27] An additional complication with model-

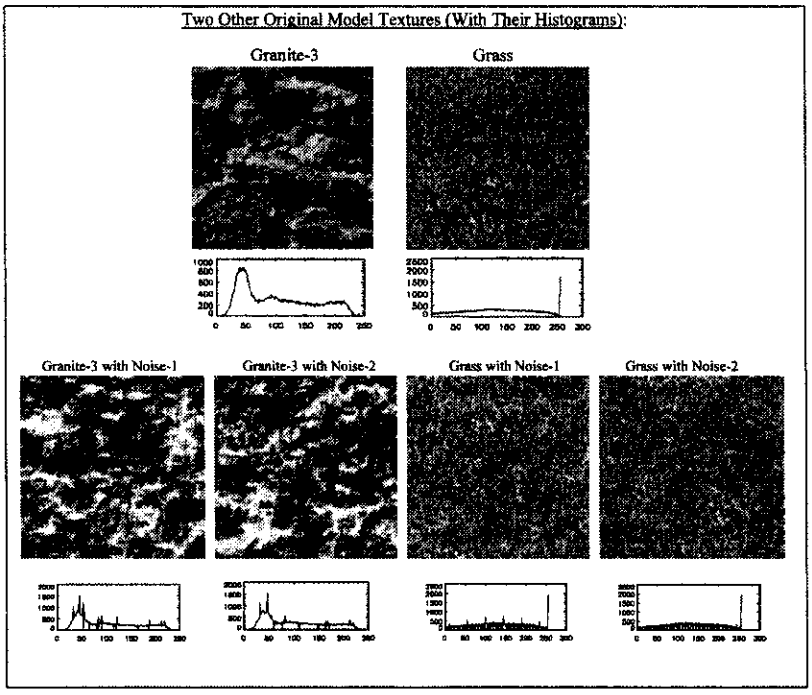

Fig. 3 Results of texture synthesis for two textures denoted as Granite-3 and Grass. The histograms of the original samples as well as of the syntheses for two realizations of uniformly distributed white noise are shown.

ing biological tissue as a fractal is that it is difficult to accurately estimate a fractal dimension from digitized data.[28]

The indication that the power spectra of mammograms and various natural images follow some power law may be significant. It is however important to note it has been demonstrated that the power spectrum of a statistical complex background is not a complete descriptor of the required background statistics to predict human observer performance in various detection tasks. Specifically, two studies demonstrate that two sets of images with equal power spectra, yet having Fourier spectra that differ in phase, yield different detectability performance and thus require different predictive mathematical models.[22,24] An ensemble of images with the same power spectrum as that of another ensemble of images but with a Fourier spectrum of random phase was obtained by filtering various realizations of white noise with the desired power spectrum.

While power spectra calculations are commonly employed to characterize complex backgrounds, it must be noted that only Gaussian random processes can be fully characterized by their first order statistics and their autocorrelation function. Knowledge of these quantities is sufficient to compute the statistical property of the random process to any order. The second order statistics, however, for non-Gaussian random processes are defined as the two-point probability density function (2P-PDF). The power spectrum computation can be conducted knowing the 2P-PDF but the reverse is not true. We are currently further investigating the relative role of power spectra versus the 2P-PDF for detection of targets in complex backgrounds with non-Gaussian statistics.

Knowing that complex backgrounds such as mammograms cannot be modeled either as a fractal or as filtered white noise to yield a given ensemble power spectrum, we propose an alternative approach to modeling such backgrounds. The model is established from knowledge of the anatomy of such tissues and their radiographic appearance.[29] Radiographic contrast in mammography arises from differing attenuation between tissues that comprise the breast. The breast is made essentially of a mixture of fatty tissue, which appears dark on radiographs, connective and epithelial tissue which produce bright radiographic appearances also referred to as mammographic densities, and prominent ducts which yield cord-like structures or a beaded appearance.[25,27]

Overall, a set of mammographic radiographs from the same type of breast tissue may be described as a stochastic process with fairly large scale structures that account for mammographic densities on black backgrounds, and smaller scale structures that give the tissue the appearance of texture. We thus propose a model that is based on the decomposition of such complex backgrounds into two components: a mean background (i.e. the slowly, spatially varying component) and a mean texture image. The background accounts for large-scale inhomogeneity in the mammographic background and the texture characterizes the fluctuations of that image around the mean background.

A realization of the mean background is typically obtained by convolving a sample of a mammographic sample image with a two-dimensional Gaussian kernel.[30,31] An example of the sample image and the resulting blurred image

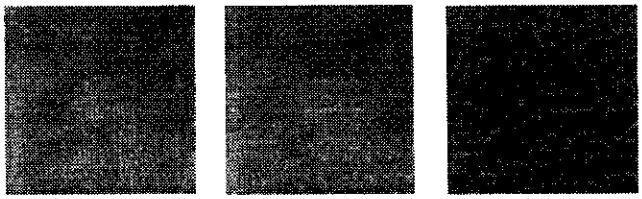

(a) (b) (c)

Fig. 4 Mammography breast image decomposition: (a) the original sample; (b) the slowly, spatially varying mean background; (c) the residual texture image.

are shown in Figs. 4(a) and 4(b), respectively. The sample image is a 256×256 pixel section extracted from a mammogram from the database of *N.* Karssemeijer of University Hospital Nijmegen, The Netherlands.[32] A sample of the residual texture image is obtained by subtracting the mean background from the original image. The residual texture image corresponding to the sample image shown in Fig. 4(a) is shown in Fig. 4(c).

We first propose to model the mean background as a lumpy background that is defined as a wide-sense stationary stochastic process with a Gaussian autocorrelation function.[1,33,34] We thus assume that the stochastic process describing an ensemble of mean backgrounds extracted from several sub-images of a set of mammograms is wide-sense stationary as well. While the validation of this assumption is ultimately required, our experience with mammograms suggests that wide-sense stationarity is a reasonable assumption to make. We propose to synthesize the texture image using a four-layer pyramid framework described earlier. Finally, we propose that various linear weighted sums of the two model components, the lumpy background and the synthesized texture, yield mammograms with typical radiographic characteristics.

While this model is being further investigated, current literature provides some support for the proposed model. First, Hunt and Cannon demonstrated that natural scenes can be decomposed into intensity fluctuations around a nonstationary ensemble mean where the mean is estimated by blurring a typical ensemble member.[30] Our model differs from that of Hunt and Cannon as we hypothesize that the mean background arises from an underlying wide-sense stationary process. Moreover, in support of this model, several investigations by Byng and colleagues suggest that at least two parameters are required to characterize mammograms: one parameter to describe the distribution of breast tissue density as reflected by the brightness of the mammograms, and another parameter to characterize the texture.[27] The mean background and texture components of the proposed decomposition are reminiscent of the first and second parameters in Byng's model, respectively.

4.1 *Synthesis of the Slowly Varying Mean Background*

We propose to model the mean background as a stochastic process known as the lumpy background which has been developed to specifically account for spatially varying backgrounds in medical images as a result, for example, of

anatomical structures.[1-3] In the case of mammography, the mean background may account for the relative amount of fat and densities in the breast tissue.

The lumpy background, detailed in Rolland,[1] was devised to be mathematically tractable for computing signal-to-noise ratio predictions for various medical imaging tasks.[1-3,34] The lumpy background is designed to be wide-sense stationary, that is, stationary over the ensemble of images, where the autocorrelation function is only a function of the shift variable r. A second important characteristic of the lumpy background is that its autocorrelation function is a Gaussian function. The power spectrum $W(\rho)$ is then defined as the Fourier transform of the autocorrelation function and is given by

$$W(\rho)=W(0)\exp(-2\pi^2 r_b^2|\rho|^2), \tag{1}$$

where ρ is the 2D frequency variable in the Fourier domain conjugate to r, r_b is the correlation length of the autocorrelation function, and $W(0)$ is the value of the power spectrum at zero frequency that we refer to as the lumpiness measure.

Two models of the lumpy backgrounds were presented in Rolland.[1] The first approach consisted of superimposing 2D Gaussian functions, referred to as Gaussian blobs, on a constant background of strength B_0. To keep the mathematics simple, we assumed 2D Gaussian blobs of constant amplitude $b_0/\pi r_b^2$ and constant half-width r_b. In this case, the lumpy background can be shown to be mathematically specified as

$$b(r)=\sum_{j=1}^{K}\frac{b_0}{\pi r_b^2}\exp\left[-\frac{|r-r_j|^2}{r_b^2}\right], \tag{2}$$

where r_j is a random variable uniformly distributed over the background area, and K is the number of Gaussian blobs in the background. Rolland further showed that to yield a Gaussian autocorrelation function, the number of Gaussian blobs K must also be a random variable with the mean of K equal to its variance. We thus chose K to be Poisson distributed for this condition to be satisfied.[1,2] A measure of lumpiness in the background is given by

$$W(0)=\frac{\bar{K}}{A_d}b_0^2, \tag{3}$$

where $\bar{K}/A_d$ is the mean number of Gaussian functions per mm^2.

By varying the background lumpiness, one can simulate various types of tissue inhomogeneities. We hypothesize that the width of the Gaussian blobs can be chosen to represent existing correlation lengths of the tissue densities in various types of tissues.

We conducted some simulations with the mammographic background where the mean background was extracted from the mammographic images by convolving the latter with a Gaussian kernel of standard deviation six pixels.[9] For the lumpy stochastic process, eighteen images were simulated of lumpiness value 10^6 counts^2/(sec^2 pixels) (i.e. mean number of blobs was 400, the strength of a blob $b0$ was 12,800 counts/sec) and of correlation length rb equal to 15 pixels. For the synthesized texture images, eighteen syntheses were obtained using three of the residual texture images from the ensemble. While the simulated lumpy backgrounds visually appeared as fairly good models of the mammographic slowly varying component, further investigations are needed to compare the underlying statistics. As discussed in Section 6, a statistical analysis leads us to also consider other models besides the lumpy backgrounds.

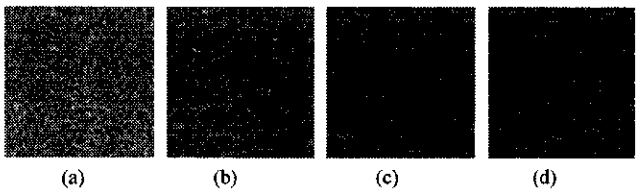

Fig. 5 Syntheses of a residual mammographic texture image: (a) a typical sample of a uniformly distributed white noise image used as a starting point for one synthesis; (b) original mammographic residual texture; (c) synthesis 1; (d) synthesis 2.

4.2 *Synthesis of the Residual Texture Image*

The framework detailed in Section 2 was applied to synthesize the residual texture component. Results of the synthesis are shown in Fig. 5. On the left, a realization of the noise is shown. It is followed to the right with the residual texture. The two rightmost images are two realizations of the synthesis corresponding to two different realizations of the noise.

5 A Proposed Mathematical Phantom

The synthesis of an ensemble of images $M_i(x,y)$ according to the described mathematical phantom can be established using an adaptive linear combination of realizations from the two model components: a realization of a lumpy background component denoted as $L_i(x,y)$ and a realization of the synthesized texture component denoted as $T_i(x,y)$. The resulting synthesized image will then be given by

$$M_i(x,y)=\beta L_i(x,y)+(1-\beta)T_i(x,y), \tag{4}$$

where β ranges from 0 to 1. Such a combination will allow us to span a wide range of tissue types with relative amounts of lumpy backgrounds and texture backgrounds. We hypothesize that by choosing the parameters of the lumpy background (i.e. correlation length and lumpiness values) and the types of texture to synthesize, various tissue types as described by Wolfe for example can be synthesized.[29] On a more theoretical basis, one can also study a wide range of combinations of such backgrounds by varying β and the parameters associated with each component. Such a framework may naturally find application to a wide range of complex backgrounds.

6 First and Second Order Statistics

It has been shown that accounting for second order statistics measured with power spectra is insufficient to predict target detectability in complex backgrounds. We are thus

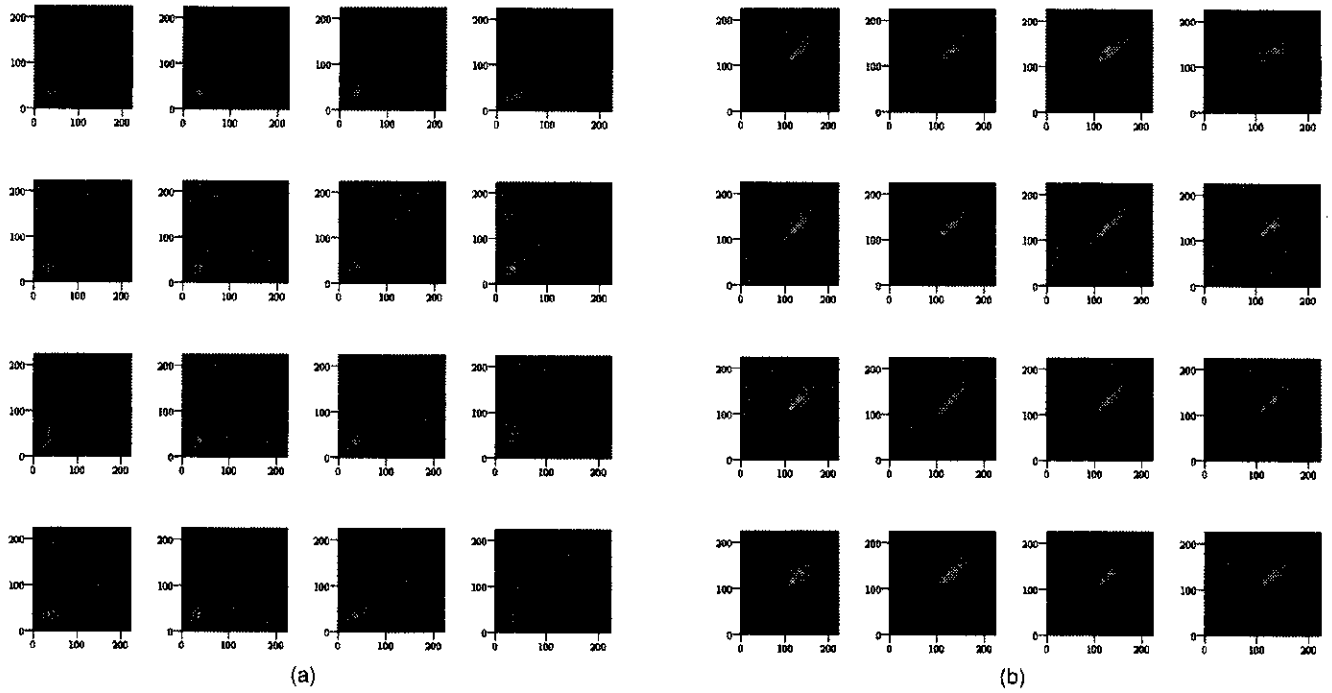

Fig. 6 (a) 2P-PDFs for Granite-1 with no histogram matched to the mammographic residue image. From upper left to upper right corners the directional distance **d** takes values of (−5,−5), (−3,−5), (3,−5), (5,−5); from top left to bottom left, **d** takes values of (−5,−5), (−5,−3), (−5,3), and (−5,5). (b) 2P-PDFs for Granite-1 with histogram matched to the mammographic residue image. From upper left to upper right corners the directional distance **d** takes values of (−5,−5), (−3,−5), (3,−5), (5,−5); from top left to bottom left, **d** takes values of (−5,−5), (−5,−3), (−5,3), and (−5,5).

investigating the complete second-order statistics of complex backgrounds as described by the 2P-PDF with the aim in mind to foster the future establishment of more effective figures of merit for target detectability in complex backgrounds.[34] The 2P-PDF and often components of the 2P-PDF are also known as the co-occurrence matrix, especially in the literature on texture segmentation. Julez first used grey tone spatial dependence co-occurrence statistics in texture discrimination experiments.[35] Various statistical measures have been extracted from the 2P-PDF for use in automatic texture discrimination.[36] The autocorrelation function has been one of the measures most widely employed in analyzing statistical backgrounds like natural scenes. For our purpose, effective detection of targets in complex textured backgrounds, we propose to work with the complete 2P-PD instead of extracted features.[36]

A 2P-PDF is computed as the frequency of simultaneous occurrence of two grey levels from two pixels separated by a directional distance **d**. A 2P-PDF is computed for each value of the vector **d**. We present computations of 2P-PDFs for some of the textures considered in this paper. For both the original mammographic texture image and its synthesis, the first order statistics were naturally matched. This also applies to the mammographic mean backgrounds and lumpy backgrounds. We then define a distance measure between two 2P-PDFs as

$$D(p^{(a)},p^{(b)})=\frac{1}{N_{\mathbf{d}}}\sum_{\mathbf{d}}\left(\sum_{ij}[(p^{(a)}(GL_i,GL_j;\mathbf{d})-p^{(b)}) \times(GL_i,GL_j;\mathbf{d})]^2\right)^{1/2}, \tag{5}$$

where ij is a pair of grey levels, $p^{(a)}$ and $p^{(b)}$ are the 2P-PDFs for texture (a) and texture (b), respectively, and $N_{\mathbf{d}}$ is the number of directional distances considered. It must be noted that D defines a distance because it satisfies the three following properties of distance:

$$\begin{aligned} &D(p^{(a)},p^{(a)})=0 \\ &D(p^{(a)},p^{(b)})=D(p^{(b)},p^{(a)}) \\ &D(p^{(a)},p^{(b)})+D(p^{(b)},p^{(c)})\geq D(p^{(a)},p^{(c)}) \end{aligned} \tag{6}$$

Computations of 2P-PDFs for some of the textures considered in this paper are shown in Figs. 6–10. It can be shown from Figs. 6(a) and 6(b) that the first order statistics have a significant impact on the form of the 2P-PDF. It can be indeed shown that in the limit of large **d** the 2P-PDF becomes the product of the 1P-PDFs (i.e. first order statistics). However, while the form of the 2P-PDF of Granite-1 resemble that of the residue image after matching of its first order statistics to that of the residue image, some asymmetry along the diagonal in the 2P-PDF can still be observed. Table 1 also confirms that the two textures are still fairly far apart compared to the distance between the residue image and its syntheses. While we do not show the 2P-PDFs for the mean and lumpy backgrounds, our investigation

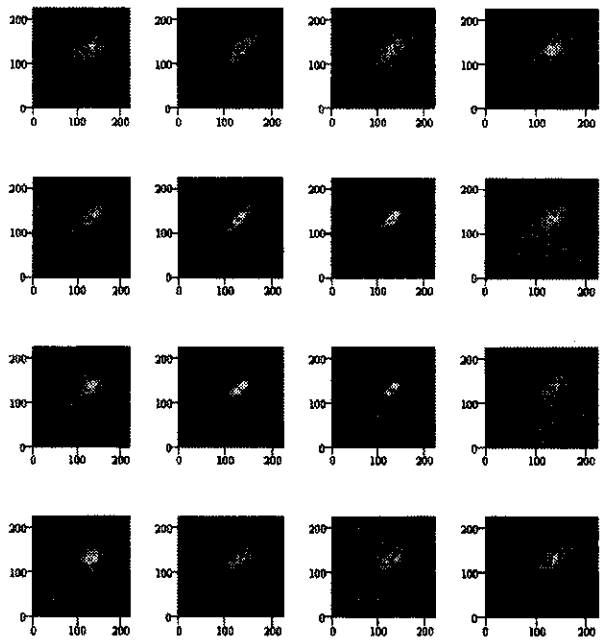

Fig. 7 2P-PDFs for Granite-2 with histogram matched to the mammographic residue image. From upper left to upper right corners the directional distance **d** takes values of (−5,−5), (−3,−5), (3,−5), (5,−5); from top left to bottom left, **d** takes values of (−5,−5), (−5, −3), (−5,3), and (−5,5).

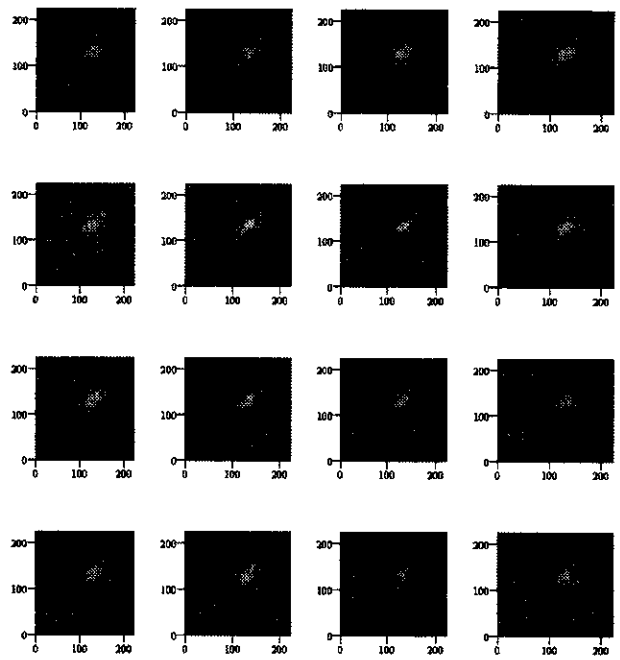

Fig. 9 2P-PDFs for the residue mammogram. From upper left to upper right corners the directional distance **d** takes values of (−5, −5), (−3,−5), (3,−5), (5,−5); from top left to bottom left, **d** takes values of (−5,−5), (−5,−3), (−5,3), and (−5,5).

yields visual good agreement. However, we also recently investigated that the mean background can be effectively synthesized using the steerable pyramid transform framework which is attractive because it provides a natural way to synthesize those backgrounds with no need to heuristically choose the best parameters of the lumpy background. Therefore we are now investigating the 2P-PDFs of those new syntheses.

The distances between various textures are given in Table 1. Some of the distance computations are conducted

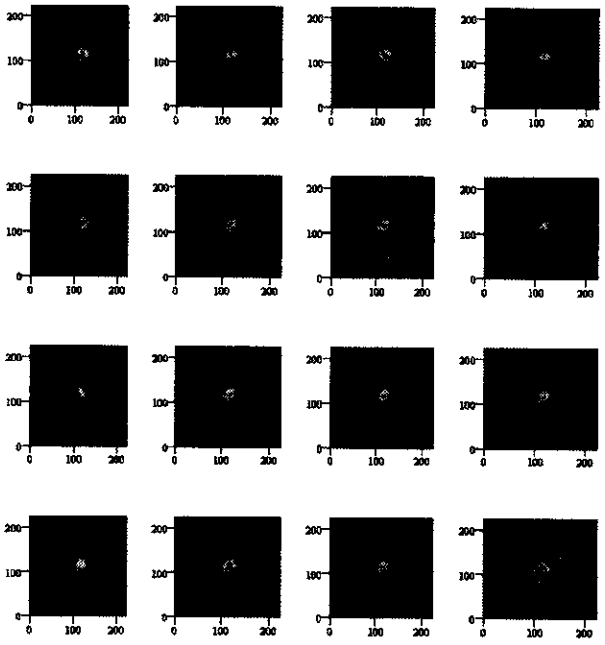

Fig. 8 2P-PDFs for Grass with histogram matched to the mammographic residue image. From upper left to upper right corners the directional distance **d** takes values of (−5,−5), (−3,−5), (3,−5), (5,−5); from top left to bottom left, **d** takes values of (−5,−5), (−5, −3), (−5,3), and (−5,5).

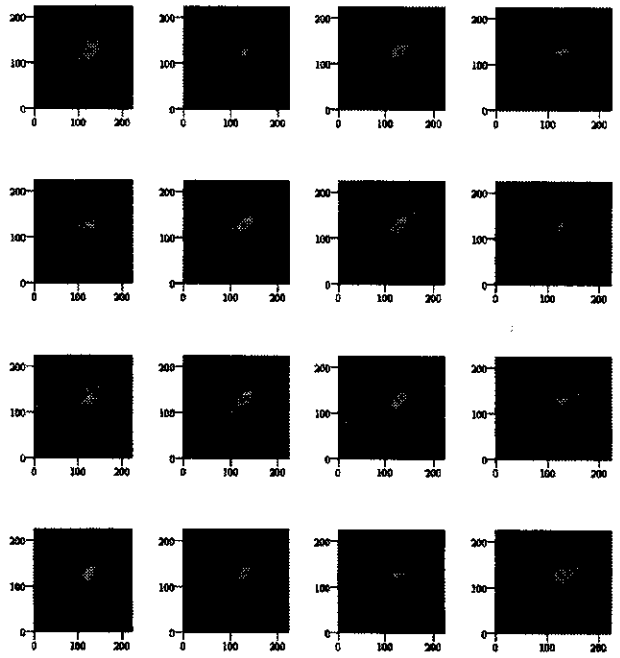

Fig. 10 2P-PDFs for the synthetic residue image with histogram naturally matched to the mammographic residue image. From upper left to upper right corners the directional distance **d** takes values of (−5,−5), (−3,−5), (3,−5), (5,−5); from top left to bottom left, **d** takes values of (−5,−5), (−5,−3), (−5,3), and (−5,5).

Table 1 Values of the distance between two 2P-PDFs are given. The measure of distance is defined by Eq. (6).

Textures	Distance
Mammo-syn1 to residue	0.618
Mammo-syn2 to residue	0.621
Mammo-syn3 to residue	0.623
Mammo-syn1 to Mammo-syn2	0.538
Granite-1 to residue	2.370
Granite-2 to residue	3.386
Granite-3 to residue	2.487
Grass to residue	2.438

after the first-order statistics of the textures were matched. For computational accuracy, all 2P-PDFs were first scaled to satisfy a normalization of 100 instead of 1. Preliminary results indicate that a small distance compared to the distance resulting from other textures separates the mammogram texture and its syntheses. Future work includes mapping the space of distances for a large number of textures and their syntheses, including white noise. This investigation is now under investigation and will be reported elsewhere.

7 Role of Background Synthesis for Effective Target Acquisition Methods

The ability to synthesize a large number of texture images that share common underlying statistical characteristics is a first step towards the extraction of effective statistical descriptions of complex backgrounds for use in specific tasks.[2,9,30,34] If the end user is a human observer, the ultimate test will be to conduct a set of psychophysical studies using real images and mathematically simulated images to validate the performance predictions. A statistical ensemble of images is required for such studies and availability of a mathematical phantom to generate an ensemble with specified targets embedded can be an effective way to conduct a large number of experiments. Such methods can be generalized to mathematical observers for automatic target acquisition.

Current state-of-the-art Figures of Merit for predicting the detection of targets in complex backgrounds that we have participated in developing include solely the computation of the covariance matrix of the underlying random process associated with the background.[34] While the covariance matrix has been extensively and is still considered for developing Figures of Merit for detection of target in textured backgrounds, we currently hold the vision that Figures of Merit based on the 2P-PDF should be considered in addition. 2P-PDFs bring forward information about the mutual spatial relationship between grey levels at multiple scales and orientation. The covariance matrix which is related to the power spectrum for stationary random processes provides only a global measure of spatial frequency content in a texture image. For nonstationary random processes, the power spectrum is not defined but the covariance matrix is and can be considered. However, the covariance matrix is only one moment of the 2P-PDF that characterizes how two pixel grey level values at two points in the image covary. The 2P-PDF to the contrary fully characterizes the second order statistics and likely provides a more powerful tool to characterize detection in complex backgrounds.

8 Conclusion

We presented a two-stage framework for the synthesis of complex texture backgrounds and demonstrated its application to the synthesis of rock, grass, and mammographic tissue. In the latter case, a tissue sample was described as the sum of a slowly, spatially varying mean background (i.e. mean background) and a residual texture image. We proposed to synthesize the mean background using a stochastic process known as the lumpy background that one of the authors (Dr. Rolland) and colleagues established in previous investigations.[3–5] The fine scale textures were synthesized using a four-layer pyramid decomposition framework we developed over the last year. The first and complete second order statistics (2P-PDFs) of the various ensembles of images were presented. A measure of distance between a pair of 2P-PDFs associated with two textures is given that may find application in texture discrimination and also target detection in such backgrounds. Work in progress in our laboratory includes development of Figures of Merit for target detection based on the 2P-PDFs.

Acknowledgments

This work was supported in part by the University of Central Florida small grant program. We are deeply thankful to Harry Barrett and Eric Clarkson for stimulating discussion with Dr. Rolland about power spectrum and 2P-PDFs characterization of textures. Finally, we thank Bryan Bloss for some assistance with IDL programming.

References

1. J. P. Rolland, "Factors influencing lesion detection in medical imaging," PhD dissertation, University of Arizona (1990).
2. K. J. Myers, J. P. Rolland, H. H. Barrett, and R. F. Wagner, "Aperture optimization for emission imaging: effect of a spatially varying background," *J. Opt. Soc. Am. A* **7**, 1279–1293 (1990).
3. J. P. Rolland and H. H. Barrett, "Effect of random background inhomogeneity on observer detection performance," *J. Opt. Soc. Am. A* **9**, 649–658 (1992).
4. G. C. Cross and A. K. Jain, "Markov random field texture models," *IEEE Trans. Patt. Anal. Mach. Intell.* **5**, 25–39 (1983).
5. R. Chellappa and R. L. Kashyap, "Texture synthesis using 2-D noncausal autoregressive models," *IEEE Trans. Acoust. Speech Sig. Proc.* **33**, 194–203 (1985).
6. J. P. Lewis, "Algorithms for solid noise synthesis," in *Computer Graphics, Proc. SIGGRAPH 89* **23**, 263–270 (1989).
7. A. Witkin and M. Kass, "Reaction-diffusion textures," in *Computer Graphics, Proc. SIGGRAPH* **25**, 299–308 (1991).
8. G. Turk, "Generating textures on arbitrary surfaces using reaction-diffusion," in *Computer Graphics, Proc. SIGGRAPH* **25**, 289–298 (1991).
9. J. P. Rolland and R. Strickland, "An approach to the synthesis of biological tissue," *Optics Express* **1**(13), 414–423 (1997).
10. D. J. Heeger and J. R. Bergen, "Pyramid-based texture analysis/synthesis," *Compt. Graph.* 229–238 (1995).
11. E. P. Simoncelli and E. H. Adelson, "Subband transforms," in *Subbands Image Coding*, J. W. Woods, Ed. Kluwer, Academic Publishers, Norwell, MA (1991).
12. E. P. Simoncelli, W. T. Freeman, E. H. Adelson, and D. J. Heeger, "Shiftable multi-scale transforms," *IEEE Trans. Info. Theory*, Special Issue on Wavelets **38**, 587–607 (1992).
13. P. Perona, "Deformable kernels for early vision," *IEEE Trans. Patt. Anal. Mach. Intell.* **17**(5), 448–499 (1995).
14. J. W. Woods, *Subband Image Coding*, Kluwer Academic Publishers, Norwell, MA (1991).
15. P. P. Vaidyanathan, *Multivariate Systems and Filter Banks*, Prentice Hall, Englewood Cliffs, NJ (1993).
16. W. T. Freeman and E. H. Adelson, "The design and use of steerable

filters," *IEEE Patt. Anal. Mach. Intell.* **13**(9), 891–906 (1991).
17. E. P. Simoncelli and W. T. Freeman, "The steerable pyramid: a flexible architecture for multi-scale derivative computation," *Proc. IEEE Int. Conf. Image Processing*, Washington DC (Nov. 1995).
18. W. K. Pratt, *Digital Image Processing*, John Wiley & Sons, New York (1991).
19. K. R. Castleman, *Digital Image Processing*, Prentice Hall, Englewood Cliffs, NJ (1996).
20. J. P. Rolland, V. Vo, C. K. Abbey, L. Yu, and B. Bloss, "An optimal algorithm for histogram matching: application to texture synthesis," (in press).
21. J. R. Bergen, David Sarnoff Research Center, Princeton, New Jersey, Personal Communication (1995).
22. M. G. A. Thomson and D. H. Foster, "Role of second- and third-order statistics in the discriminability of natural images," *J. Opt. Soc. Am. A* **14**(9), 2081–2090 (1997).
23. C. Caldwell and M. Yaffe, "Fractal analysis of mammographic parenchemal pattern," *Phys. Med. Biol.* **35**, 235–247 (1990).
24. F. O. Bochud, F. R. Verdun, C. Hessler, and J. F. Valley, "Detectability on radiological images: the influence of anatomical noise," *Proc. SPIE* **2436**, 156–165 (1995).
25. B. Zheng, Y. H. Chang, and D. Gur, "Adaptive computer-aided diagnosis scheme of digitized mammograms," *Acad. Radiol.* **3**(10), 806–814 (1996).
26. M. F. Barnsley, *Fractals Everywhere*, Academic Press, San Diego, CA (1988).
27. J. W. Byng, M. J. Yaffe, G. A. Lockwood, L. E. Little, D. L. Tritchler, and N. F. Boyd, "Automated analysis of mammographic densities and breast carcinoma risk," *Cancer* **80**(1), 66–74 (1997).
28. B. Dubuc, C. R. Carmes, C. Tricot, and S. W. Zucker, "The variation method: a technique to estimate the fractal dimension of surfaces," *Proc. SPIE* **845**, 241–248 (1987).
29. J. N. Wolfe, "Breast patterns as an index of risk for developing breast cancer," *Am. J. Roentgenol.* **126**, 1130–1139 (1976).
30. B. R. Hunt and T. M. Cannon, "Nonstationary assumptions for Gaussian models of images," *IEEE Trans. Sys. Man Cybern.*, 876–882 (1976).
31. R. N. Strickland and H. I. Hahn, "Wavelet transforms for detecting microcalcifications in mammograms," *IEEE Trans. Med. Imaging* **15**, 218–229 (1996).
32. The Nijmegen database is available by anonymous FTP from ftp://figment.csee.usf.edu/pub/mammograms/nijmegen-images.
33. A. Papoulis, *Probability, Random Variables, and Stochastic Processes*, McGraw-Hill, New York (1991).
34. H. H. Barrett, J. Yao, J. P. Rolland, and K. J. Myers, "Model observers for assessment of image quality," *Proc. Natl. Acad. Sci. USA* **90**, 9758–9765 (1993).
35. B. Julez, "Visual pattern discrimination," *IRE Trans. Inform. Theory* **8**(2), 84–92 (1962).
36. R. M. Haralick, "Statistical and structural approaches to texture," *Proc. IEEE* **67**(5), 786–804 (1979).

Jannick P. Rolland is assistant professor at the School of Optics and Center for Research and Education in Optics and Lasers (CREOL) at the University of Central Florida in Orlando. She received an advanced engineering degree from l'Ecole Superieure D'Optique in Orsay, France in 1984 and her PhD from the Optical Sciences Center at the University of Arizona in 1990. During her doctorate education, she conducted research in optical system design, optical testing, and image understanding. She developed some statistical models of complex backgrounds known as the lumpy backgrounds. Such background models have been widely employed in developing predictive models of tasks performance in complex backgrounds. In 1990, she joined the Department of Computer Science at the University of North Carolina at Chapel Hill to investigate some off-axis head-mounted display design for augmented reality medical application. She also worked with the Vision Research Group and developed modeling software for realistic angiograms based on methods known in differential geometry. She was appointed head of the Vision Research Group in 1992 and pursued her research in image understanding and technologies for virtual reality environments, including studies of perception in such environments. Because of her deep love for optics and how it crosses other disciplines, she decided to join CREOL in 1996. She currently enjoys teaching geometrical optics, optical system design, and technologies for virtual environments. Her current research interests aim at the development and assessment of effective technologies for 3D imaging and visualization, especially as they relate to medical and biomedical.

Alexei A. Goon is an exchange student at CREOL at the University of Central Florida in Orlando. He was the winner of all Russia theoretical mechanics and physics competitions. As a result he received a Russian government scholarship to come and study in the United States. His current research interests are in biomedical optics, ultra fast spectroscopy of chemical processes, and image analysis.

Liyun Yu: Biography and photograph not available.